

Numerical Wave Modeling based on Curvilinear Element Meshes

V. Berkhahn

Institute for Computer Science in Civil Engineering, University of Hannover, Germany

S. Mai

Franzius-Institute for Hydraulic and Coastal Engineering, University of Hannover, Germany

ABSTRACT: The results of numerical wave simulations are strongly influenced by the type and the resolution of the computational mesh representing the bathymetry. Especially in coastal areas best results in wave hindcast are acquired using curvilinear meshes as revealed by an analysis of wave propagation in the estuary of the river Ems at the German North Sea Coast. An innovative method to generate curvilinear as well as rectangular meshes is based on approximation of the bathymetry using an adapted b-splines technique. This approach fits free form surfaces to measurements. Its requirements are outlined putting emphasis on the mathematical formulation.

1 INTRODUCTION

Numerical simulations in coastal hydrodynamics based on the methods of finite differences require regular element meshes of bathymetry. Traditionally these meshes are created by interpolation techniques like triangulation or kriging. Alternatively meshes may be created by the approximation of the bathymetry with free form surfaces, e.g. b-spline surfaces (Berkhahn 2002). The latter technique is especially favorable when using curvilinear finite element meshes. The type and the resolution of the computational meshes strongly influences the results of numerical simulations as modeling of wave propagation within the estuary of the river Ems at the German North Sea coast reveals. Within a focus area in the Ems estuary nested models are set-up to analyze the effect of different bathymetric meshes. At three locations within the focus area the wave parameter and spectra are evaluated.

2 THEORETICAL BACKGROUND OF B-SPLINE SURFACES

The generation of bathymetric meshes is carried out applying the b-spline technique widely used in computer aided geometric design and re-engineering of surfaces. A point on a b-spline surface is defined by

$$\mathbf{b}(u, v) = \sum_{i=0}^N \sum_{j=0}^M \mathbf{d}_{ij} N_i^K(u) N_j^L(v) \text{ for } u \in [u_K, u_{N+1}] \text{ and } v \in [v_L, v_{M+1}] . \quad (1)$$

In equation (1) all expressions in bold face indicate a point in the three-dimensional Euclidian space E^3 . On the left hand side of this equation $\mathbf{b}(u, v)$ denotes a point on the b-spline surface in dependence of the two parameters u and v . The first expression \mathbf{d}_{ij} in the double sum describes a regular grid of $N+1$ control points in u parameter direction and $M+1$ control points in v parameter direction. Often these control points are called de Boor points. The shape functions in u and v parameter directions are called b-spline functions $N_i^K(u)$ and $N_j^L(v)$, where the upper indices K and L indicate the degree of the b-spline functions.

The parameters u_i and u_{i+1} denote the lower and upper bounds of the i^{th} parameter interval. All bounds of the parameter intervals are gathered in the knot vector \mathbf{u}

$$\mathbf{u} = [u_0, \dots, u_{N+K+1}]^T \quad . \quad (2)$$

In order to ensure the property of local modeling possibility, the influence of the control points with respect to the shape of the surface has to be restricted to a specified parameter range. Therefore the b-spline functions of degree 0 are defined as follows

$$N_i^0(u) = \begin{cases} 1 & \text{for } u \in [u_i, u_{i+1}[\\ 0 & \text{else} \end{cases} \quad \text{for } i = 0, \dots, N + K \quad . \quad (3)$$

The b-spline functions of higher degree are given with the recursive formula

$$N_i^r(u) = \frac{u - u_i}{u_{i+r} - u_i} N_i^{r-1}(u) + \frac{u_{i+r+1} - u}{u_{i+r+1} - u_{i+1}} N_{i+1}^{r-1}(u) \quad \text{for } \begin{matrix} r = 1, \dots, N + K \\ i = 0, \dots, N + K - r \end{matrix} \quad . \quad (4)$$

The b-spline function N_i^r of degree r is based on the b-spline functions N_i^{r-1} and N_{i+1}^{r-1} which ensures the important property of local modeling possibility

$$N_i^r(u) = 0 \quad \text{for } u \in R \setminus]u_i, u_{i+r+1}[\quad . \quad (5)$$

The equation (1) has to be an affine combination. This requirement is fulfilled only within the interval

$$\sum_{i=0}^N N_i^K(u) = 1 \quad \text{for } u \in [u_K, u_{N+1}] \quad , \quad (6)$$

which leads to the restriction for the parameters u and v in equation (1).

3 BATHYMETRY APPROXIMATION

The boundary control points of the regular control point grid \mathbf{d}_{ij} in equation (1) are generated within the meshing tool HydroMesh (Göbel 2004) by means of b-spline curves. The interior control points are generated with the Coons interpolation method. In the case of the Ems estuary this leads to the control grid indicated in Figure 1. After this editing process the control point grid is generated in the plane $z = 0.0$ and the realistic z -coordinates of all control points are still unknown. The adaptation of this initial control grid is performed with an efficient iteration algorithm (Berkhahn & Mai 2004) and yields to the three-dimensional distribution of the adapted control point grid illustrated in Figure 1.

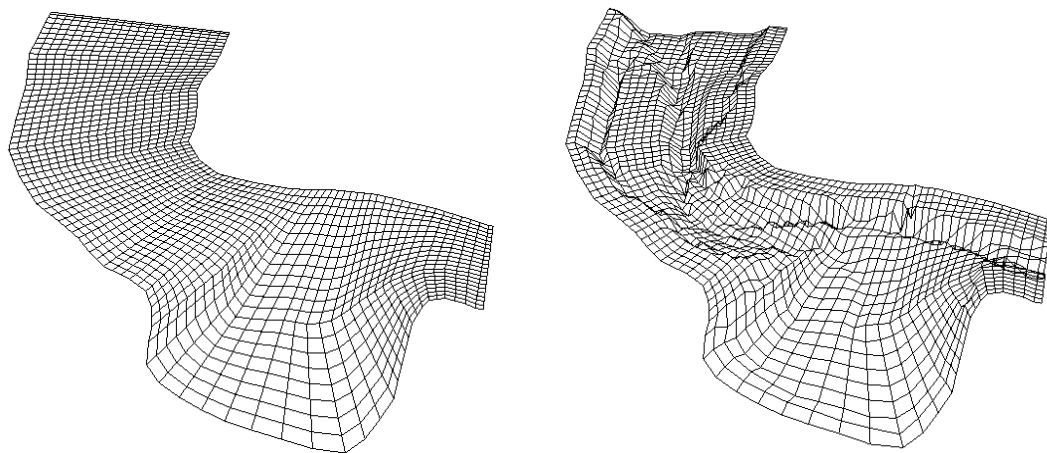


Figure 1. Control points grid of the Ems estuary created with HydroMesh; initial control point grid in the xy -plane (left) and adapted control point grid in the E^3 space (right)

4 MESH GENERATION

Since the approximating b-spline surface is based on a regular de Boor point grid it is very easy to generate a regular quadrilateral element mesh. The element nodes \mathbf{n}_{ij} are generated in the uv -parameter space of the b-spline surface with equal parameters distances Δu and Δv . With equation (1) the element nodes \mathbf{n}_{ij} are determined in the three-dimensional Euclidian space E^3

$$\mathbf{n}_{ij} = \mathbf{b}(u_0 + i\Delta u, v_0 + j\Delta v) \quad . \quad (6)$$

The methods of free form surface modeling are implemented into the tool HydroMesh (Göbel 2004). This tool is used to create various rectangular and curvilinear bathymetric meshes of different resolutions within the focus area. Examples of these meshes are given in Figure 2. The element mesh size is set to 50×40 , 100×80 , 200×160 and 400×320 for rectangular meshes and to 20×80 , 40×160 , 80×320 and 160×640 for curvilinear meshes.

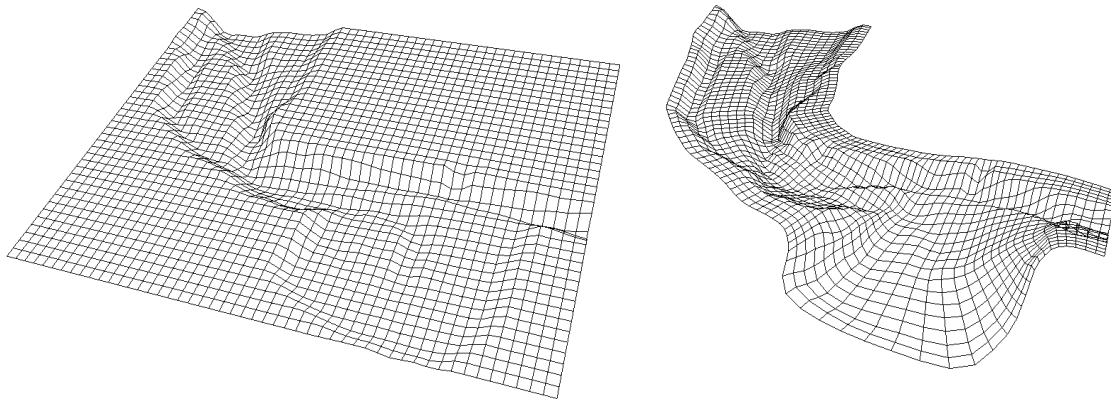


Figure 2. Orthogonal element mesh with size 50×40 (left) and curvilinear element mesh with size 20×80 (right) created with HydroMesh

5 WAVE MODEL

For the different computational meshes wave simulations are carried out using the phase-averaged model SWAN (Booij et al. 1999, Ris et al. 1999) in its stationary mode. The basis of SWAN operated in the stationary mode is the action balance equation

$$\frac{\partial}{\partial x} c_x N + \frac{\partial}{\partial y} c_y N + \frac{\partial}{\partial \sigma} c_\sigma N + \frac{\partial}{\partial \theta} c_\theta N = \frac{S}{\sigma} \quad . \quad (7)$$

The first and the second term on the left hand side represent the propagation of action in geographical space (with propagation velocities c_x and c_y in x - and y -space). The third term describes the frequency shift due to variations in depths (with propagation velocity c_σ in σ -space). The fourth term models the depth-induced refraction (with propagation velocity c_θ in θ -space). The right hand side of the action balance equation is the source respectively sink term of energy density representing the effects of generation, dissipation and nonlinear wave-wave interactions. Equation (7) is discretized in σ -, θ -space as well as in x -, y -space using the computational mesh derived by b-spline surfaces.

The incoming wave conditions at the northern boundary of these models are derived via nesting into a coarse large scale model for boundary conditions of water levels from 3 m to 5 m above mean sea level and wind speeds from 8 m/s to 32 m/s with directions from 0° to 360° . Figure 3 exemplifies this approach presenting also a comparison of modeling results calculated with a fine rectangular and a fine curvilinear mesh respectively. Although the wave field is comparable for both mesh types differences in significant wave heights are found in the direct vicinity of the deeper shipping channels, e.g. near location L2.

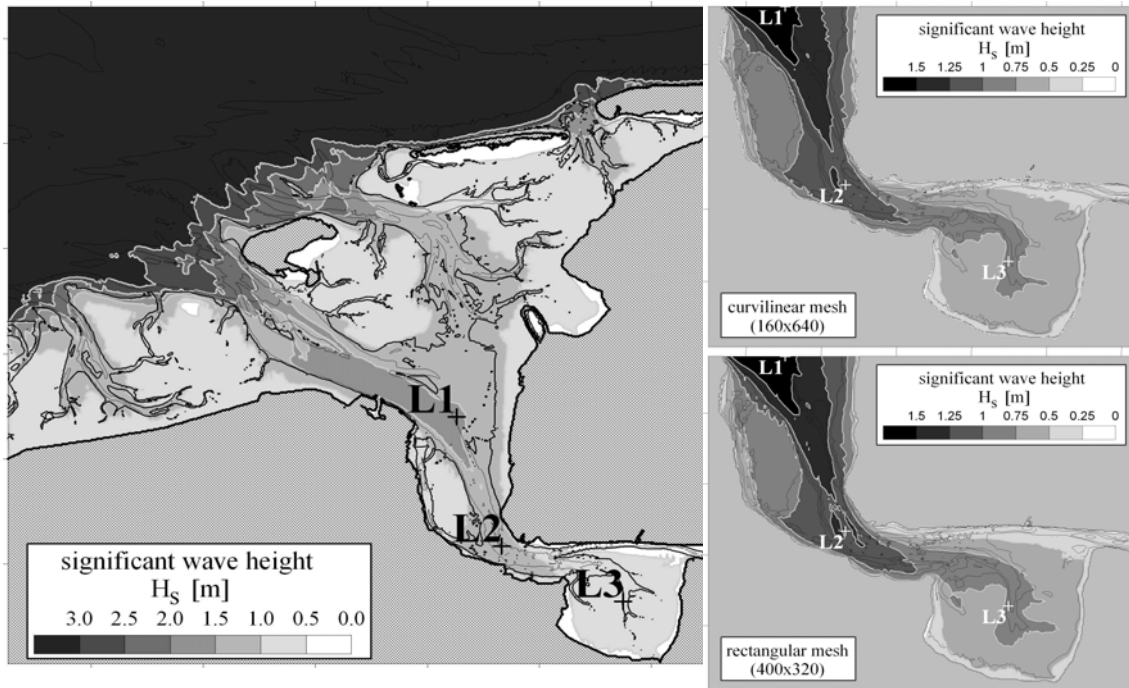


Figure 3. Wave propagation in the estuary of the river Ems: coarse model (left) and nested models with different mesh types (right); water level 3 m a. mean sea level (msl), wind 24 m/s, 300°.

6 RESULTS

The evaluation of significant wave height and mean wave period at the locations L1-L3, as given in Figure 4 and 5, reveals an overestimation of these parameters for coarse meshes.

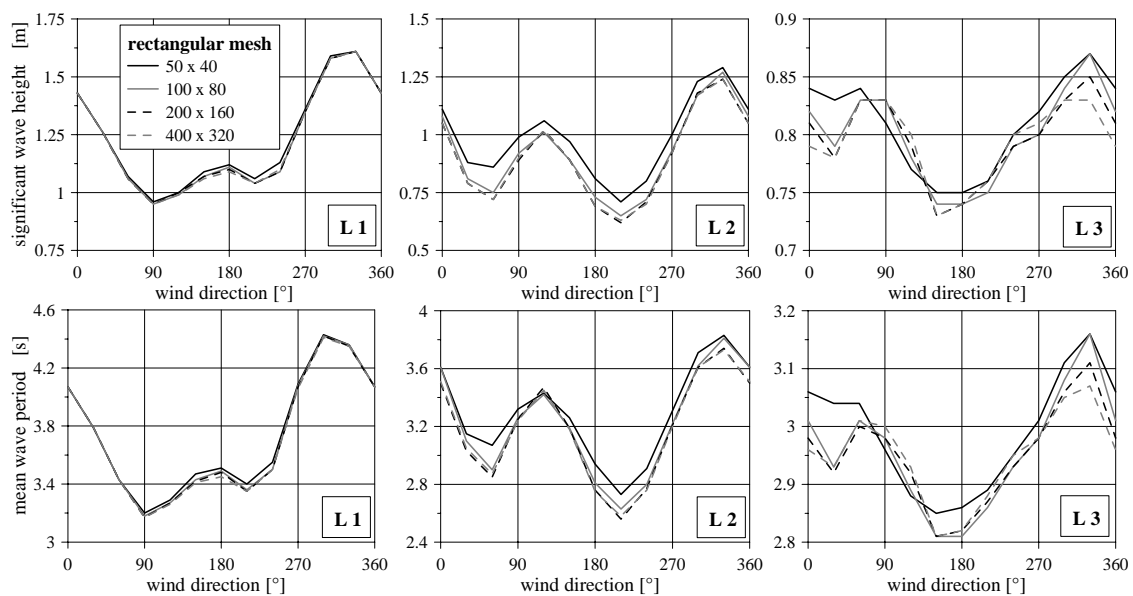


Figure 4. Significant wave height H_s and mean wave period $T_{0,1}$ at three different locations (L1-L3) within the estuary of the river Ems calculated using rectangular meshes of different resolution; water level 3 m a. msl, wind speed 24 m/s.

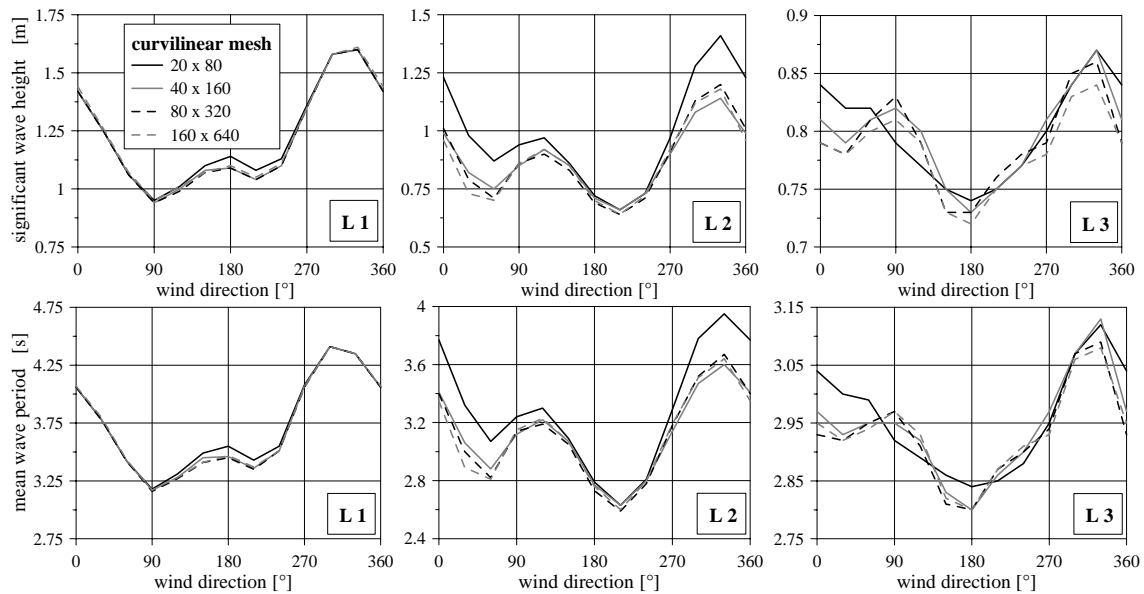


Figure 5. Significant wave height H_s and mean wave period $T_{0,1}$ at three different locations (L1-L3) within the estuary of the river Ems calculated using curvilinear meshes of different resolution; water level 3 m a. msl, wind speed 24 m/s.

The amount of overestimation increases with distance from the model boundaries (Mai & Berkahn 2003). Models with rectangular computational meshes seem to be more sensitive to resolution than curvilinear meshes as results of modeling based on curvilinear meshes converge much faster with increasing resolution. The differences in the characteristic wave parameters relate to differences in the wave spectra (Berkahn & Mai 2004) as given in Figure 6. Especially for frequencies lower than the peak frequency an overshoot in spectral density $S(f)$ is found when using coarse computational curvilinear meshes.

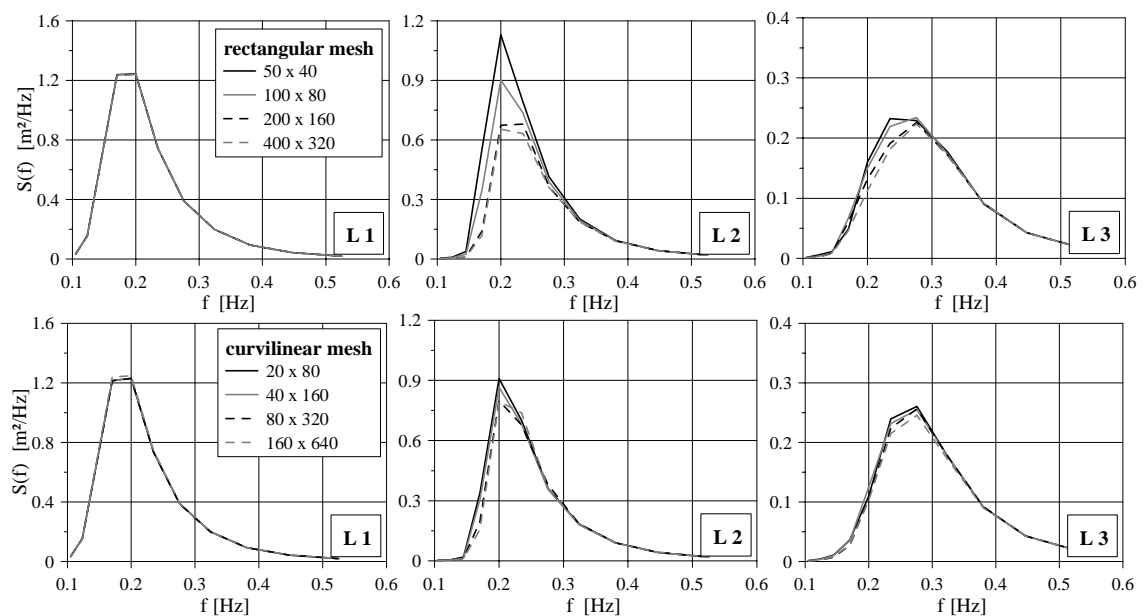


Figure 6. Wave spectra at three different locations (L1-L3) within the estuary of the river Ems calculated using rectangular (top) and curvilinear meshes (bottom) of different resolution; water level 3 m a. msl, wind 24 m/s, 300°.

7 CONCLUSION

The type of computational meshes as well as its resolution strongly influence the results of phase-averaged wave modeling. The model results converge faster when using curvilinear element meshes instead of rectangular meshes. For curvilinear meshing the theory of b-spline approximation, as realized in the tool HydroMesh, turned out to be very feasible.

REFERENCES

- Berkhahn, V. 2002. Mesh generation for hydrodynamic simulations. *Fundamentals and applications of computer science in civil engineering – state of the art in Germany; Proc. symp., University of Science and Technology, Building and Housing Research Center, Teheran, Iran, 19-20 May 2002*: 277-295.
- Berkhahn, V. & Mai, S. 2004. Meshing bathymetries for numerical wave modeling. In S.-H. Liong, K.-K. Phoon & V. Babovic (eds), *Hydroinformatics; Proc. of the 6th int. conf., Singapore, 21-24 June 2004*: 47-54. Singapore: World Scientific.
- Booij, N., Ris, R.C. & Holthuijsen, L.H.A. 1999. Third-Generation Wave Model for Coastal Regions, 1. Model Description and Validation. *Journal of Geophys. Res.* 104: 7649-7666.
- Göbel, M. 2004. Meshing Tool HydroMesh. In Projektionisten GmbH (ed.), <http://www.HydroMesh.com>.
- Mai, S. & Berkhahn, V. 2003. Generation of regular meshes for numerical wave modelling. In J. Ganoulis & P. Prinos (ed.), *Water engineering and research in a learning society: modern developments and traditional concepts; Intern. Association of Hydraulics Engineering and Research, Proc. of the XXX int. Congr., Thessaloniki, Greece, 24-29 August 2003*: D223-D230.
- Ris, R.C., Holthuijsen, L.H. & Booij, N. 1999. A third-generation wave model for coastal regions, 2. Verification. *Journal of Geophys. Res.* 104: 7667-7681.